Atmos. Meas. Tech., 3, 507–521, 2010
www.atmos-meas-tech.net/3/507/2010/
doi:10.5194/amt-3-507-2010

Atmospheric
Measurement
Techniques

μDirac: an autonomous instrument for halocarbon measurements

B. Gostlow[1], A. D. Robinson[1], N. R. P. Harris[1], L. M. O'Brien[1], D. E. Oram[2], G. P. Mills[2], H. M. Newton[2], S. E. Yong[3], and J. A Pyle[1,4]

[1]Centre for Atmospheric Science, Department of Chemistry, University of Cambridge, Lensfield Road, Cambridge, CB2 1EW, UK
[2]School of Environmental Sciences, University of East Anglia, Norwich, NR4 7TJ, UK
[3]Malaysian Meteorological Department, Ketua Stesen GAW Lembah Danum, Malaysia
[4]National Centre for Atmospheric Science, NCAS-Climate, UK

Received: 10 August 2009 – Published in Atmos. Meas. Tech. Discuss.: 11 September 2009
Revised: 19 March 2010 – Accepted: 5 April 2010 – Published: 29 April 2010

Abstract. We describe a new instrument (μDirac) capable of measuring halocarbons in the atmosphere. Portability, power efficiency and autonomy were critical design requirements and the resulting instrument can be readily deployed unattended on a range of platforms: long duration balloon, aircraft, ship and ground-based stations. The instrument is a temperature programmed gas chromatograph with electron capture detector (GC-ECD). The design requirements led to μDirac being built in-house with several novel features. It currently measures a range of halocarbons (including short-lived tracers having biogenic and anthropogenic sources) with measurement precision relative standard deviations ranging from ± 1% (CCl_4) to ± 9% (CH_3I). The prototype instrument was first tested in 2005 and the instrument has been proved in the field on technically challenging aircraft and ground-based campaigns. Results from an aircraft and a ground-based deployment are described.

1 Introduction

Halocarbons in the atmosphere were first observed by Lovelock (1971) using a gas chromatograph (GC), after his invention of the electron capture detector (ECD – Lovelock and Lipsky, 1960; see also Morris and Ettre, 2007). His initial atmospheric use for his GC-ECD was to measure CFC-11 and CFC-12, but it was soon also used to measure CH_3I and CCl_4 in air and water (Lovelock et al., 1973). Since those early beginnings, observations of atmospheric halocarbons have proven essential to improving our understanding of the interplay between different atmospheric processes in many regions of the atmosphere. Due to the wide range of atmospheric lifetime (hours to centuries) and varied sources (natural and anthropogenic; marine and terrestrial), halocarbons are valuable in tracing air mass origins and understanding dynamical and chemical processes. Observations of short-lived compounds can reveal the presence of biogenic sources (e.g. oceanic, biomass burning).

Measurements of halocarbons have been made primarily with GC-ECDs or with GC-mass spectrometers (GC-MS – e.g. Miller et al., 2008). These have been operated in the field or by collecting whole air or adsorbed air samples with subsequent measurement in the laboratory. Observations have been made routinely at ground locations for many years (Montzka et al., 1999; Prinn et al., 2000). Measurements at sea are less regular (e.g. Penkett et al., 1985; Class et al., 1986; Butler et al., 2007). Airborne (aircraft and balloon) measurements of long and short-lived halocarbons provide information on the extent and composition of the boundary layer and its impact on the tropopshere (e.g. Blake et al., 2001, Colman et al., 2001). Information about polar ozone loss (e.g., Proffitt et al., 1990; 1993), the polar vortex chemical composition and dynamics (e.g., Schmidt et al., 1994; Ray et al., 2002), the tropical tropopause layer (TTL) and its two-way transport with the stratosphere (e.g., Volk et al., 1996), and about transport in the tropopause region (e.g., Ray et al., 1999) can all be obtained by studying the distribution of halocarbon tracers. In each case the specific techniques employed have their own advantages and disadvantages. In general, the instruments deployed all require a degree of human intervention and none of the instruments can really be considered lightweight. Improved ease of use, flexibility and

---

Correspondence to: N. R. P. Harris
(Neil.Harris@ozone-sec.ch.cam.ac.uk)

Table 1. μDirac target compounds and measurement performance during the Cape Verde ground-based and aircraft campaign.

Compound name	Formula	Atmospheric lifetime	Conc. in NOAA cylinder (ppt)[a]	Scale uncertainty (%)[b]	Ground-based precision (%)[c]	Airborne precision (%)[d]	Limit of detection (ppt)[e]
methyliodide	CH_3I	5 days	3.4	20	9.3	20.2	0.5
chloroform	$CHCl_3$	5–6 months	9.93	5.0	4.0	8.1	0.5
methylchloroform	CH_3CCl_3	5 years	17.84	2.5	2.6	3.3	0.25
carbontetrachloride	CCl_4	26 years	95.0	2.0	1.1	1.9	0.1
dibromomethane	CH_2Br_2	3–4 months	4.8	10	5.4	5.7	0.15
tetrachloroethene	C_2Cl_4	3–4 months	2.01	10	4.2	8.2	0.05
bromoform	$CHBr_3$	26 days	9.0	10	4.5	17.3	0.25

[a] ppt dry air mole fraction, certified at time of filling in Dec 2005;
[b] uncertainty estimate (2 s.d.) of NOAA-ESRL calibration air;
[c] 1 s.d. of 6 calibration chromatograms made in a single day;
[d] 1 s.d. of all airborne calibrations from the Dornier aircraft flight on 1st June 2007;
[e] based on signal to noise ratio of 10.

reliability as well as lower cost are all desirable. These qualities are the rationale in the development of micro-GCs (Tienpont et al., 2009).

Here we present a new micro-GC designed to meet the need for more flexible, autonomous, low power halocarbon analysis suited to a range of field deployments. It was originally designed for use on Montgolfier Infra Rouge (MIR) long duration balloons (Pommereau and Hauchecorne, 1979; Pommereau et al., 2002), and so the discussion of the design is based around meeting those challenging requirements. However, it has proven versatile and has also been used in aircraft and ground-based deployments. This new instrument has evolved from our earlier DESCARTES and DIRAC instruments (Danis et al., 2000; Robinson et al., 2000) whose CFC measurements have been used for the estimation of Arctic ozone loss (Robinson et al., 2005) and its effect on mid-latitudes (Ross et al., 2004), and for satellite validation (Urban et al., 2005). The instrument is based on a GC-ECD system and is capable of making measurements of halocarbons with a range of atmospheric lifetimes and sources, including a number of short-lived gases such as $CHCl_3$, CH_2Br_2, C_2Cl_4, $CHBr_2Cl$, $CHBr_3$ and CH_3I. These compounds are found in the atmosphere with concentrations at and below the part-per-trillion (ppt) level (Table 1). The flexible, lightweight and autonomous design of μDirac means that a range of uses can be envisioned, with only relatively minor adaptations being required. In this paper we describe in Sect. 2 the core GC instrument which is common to all deployment scenarios. At the end of Sect. 2 we describe instrument adaptations which are specific to the type of deployment: MIR long-duration balloon; lower tropospheric aircraft and ground-based campaigns. Section 3 discusses instrument performance in terms of measurement accuracy, separation ability, precision and sensitivity. Recent deployment results are presented in Sect. 4.

2 Instrument description

μDirac is a gas chromatograph with electron capture detector which makes in situ measurements of halocarbons. To meet the exacting requirements of flight on MIR balloons it is lightweight, low power and able to operate autonomously for several weeks; as such it has been almost completely designed and made in-house. Section 2.1 describes the instrument core which is common to all uses. Specific requirements for MIR balloon, aircraft and ground-based deployments are presented in Sect. 2.2–2.4.

2.1 Core GC

The core GC is modular in design and consists of: an inlet manifold for selection of sample/calibration air or helium purge gas; a sample adsorption/desorption system; a temperature programmed column for separation; an ECD for detection (Fig. 1). Nitrogen and helium carrier gases are pressure-controlled as is the detector cell. Sample/calibration air passes through an adsorbent tube which removes halocarbons from the flow stream. After the sample has been collected, the adsorbent tube is flash heated and the desorbed halocarbons are passed through a chromatographic column with temperature and flow programming capability. After separation in the column, the target compounds pass through the ECD. The absolute calibration is determined by reference to calibration standards prepared by the National Oceanic & Atmospheric Administration (NOAA) at the Earth System Research Laboratory (ESRL). The overall time resolution is determined by the optimised GC method and is typically 8–15 min depending on the range of species being measured (Fig. 2). We now describe each element of the core GC in more detail.

Inlet manifold. This consists of: three solenoid valves acting as stream selectors; a 6 port 2 position valve (Valco Instruments Co. Inc.); a flow isolation solenoid valve; a

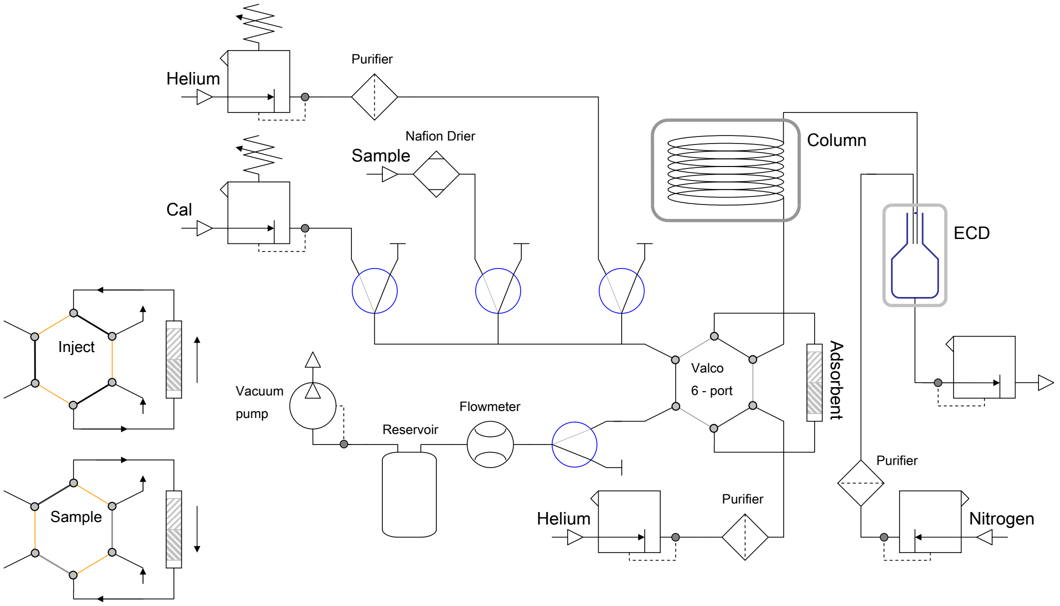

Fig. 1. Schematic of the core μDirac gas chromatograph. The smaller schematics in the lower left show the Valco valve flow paths for the "inject" and "sample" positions.

flow meter for volume determination. The stream selector valves allow input of sample air, calibration air or helium purge gas. The helium purge gas passes through a purifier tube packed with molecular sieve 13X and SK4 charcoal to remove moisture and other contaminants. The solenoid valves are mounted on custom made PEEK manifolds. The Valco valve is actuated by a model aeroplane servo motor. Downstream of the Valco valve, a solenoid valve directs flow through the flow meter until the target volume is reached. All tubing used on the inlet manifold is 1/32″ OD, 0.020″ ID PEEK.

The inlet lines for all instruments are high purity PFA tubing. The PFA tubing was tested for wall loss by flowing calibration air through a 100 foot length at ∼0.5 l min^{-1}. No significant loss of target compounds was observed. Tests using high purity nitrogen (2 min tube residence time) showed no significant contamination other than a slight memory effect for tetrachloroethene which anyway diminished with time.

Sample adsorption/desorption system. Halocarbons present in the sample (or calibration) air pass through the inlet manifold to the Valco valve. Mounted across the valve is an adsorbent tube made from a 200 mm length (0.8 mm OD, 0.53 mm ID) of methyl deactivated metal tubing. The tube contains two beds of carbon molecular sieve adsorbent (∼1 mg of Carboxen™ 1016 and ∼1 mg Carboxen™ 1001). Sample air reaches the bed of Carboxen™ 1016 first and this preferentially retains compounds with a high boiling point. Compounds with a low boiling point break readily through the Carboxen™ 1016 but are retained by the Carboxen™ 1001. The adsorption stage is typically performed within a temperature range of 15 to 25 °C.

Prior to desorption the tube is purged with helium to remove oxygen. The metal absorbent tube is flash heated resistively (typically 190 °C for 15 seconds) in a reverse flow of helium carrier gas. The tube has a mass of ∼0.35 g and resistance of ∼550 mΩ, and with over 100 W available the tube reaches the set-point temperature in about 0.5 s. The adsorbent tube temperature is calculated from the resistance which is maintained to within ∼1 mΩ of the set point until the flash period is complete. The target compounds are rapidly desorbed and pass with the helium carrier flow into the column.

Laboratory breakthrough volume tests on a new adsorbent tube showed no significant breakthrough of target compounds for sample volumes up to 500 cm^3. Our sample and calibration flows are matched to minimise any possible influence of flow (typical adsorption flow rate 10 cm^3 min^{-1}). Although the flow rate dependency of breakthrough volume has not yet been examined systematically, modelling of the passage of the sample gases through the absorbent trap indicates that breakthrough is not a problem for the gases discussed here. Breakthrough volumes are likely to be lower for older tubes which have been used continuously for several months.

The desorption efficiency has been obtained by comparing peak heights of target compounds in a calibration chromatogram with those observed in a following blank chromatogram (only He purge gas sampled). The desorption efficiency is compound specific and ranges from 85 to 98% (Table 2).

Temperature programmed column. The capillary column is a 10 m long (0.18 mm ID) Restek MXT502.2. This Silcosteel treated stainless steel column has an inner wall coating of Crossbond® diphenyl/dimethyl polysiloxane

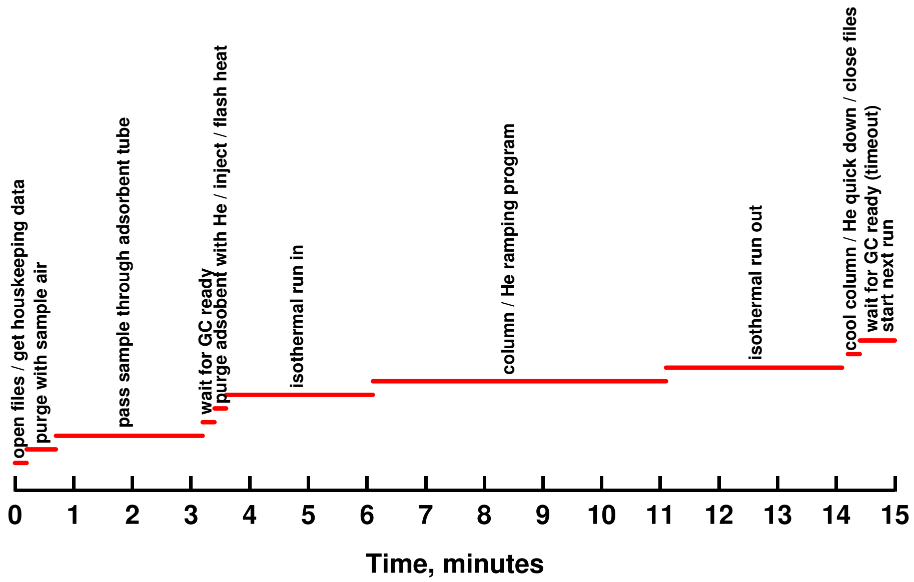

Fig. 2. The various stages of the GC method for a typical μDirac chromatogram, shown here with a 15 min overall cycle time.

Table 2. Typical desorption efficiency and chromatographic performance for μDirac target compounds.

Compound name	Formula	Desorption efficiency @ 190 °C, 15 s	Typical column RT, min	Typical SNR per ppt[a]	Peak asymmetry at half peak height[b]
methyliodide	CH_3I	86%	2.72	14	1.10
chloroform	$CHCl_3$	94%	3.95	16	1.12
methylchloroform	CH_3CCl_3	98%	4.21	28	1.03
carbontetrachloride	CCl_4	99%	4.39	77	0.79
dibromomethane	CH_2Br_2	85%	5.12	41	1.01
tetrachloroethene	C_2Cl_4	98%	6.02	170	1.07
bromoform	$CHBr_3$	94%	7.22	30	1.07

[a] based on 20 cm^3 of NOAA-ESRL calibration air;
[b] values >1 are tailed peaks, values <1 are fronted.

phase with a film thickness of 1 µm. The column is mounted in an armature consisting of two anodised aluminium end plates held apart by Vespel spacers. The column is double wound and supported by a series of Teflon "combs". The armature and column together have a mass ∼40 g. The column is connected to the Valco valve and ECD using Silcosteel® treated stainless steel tubing (0.18 mm ID). Direct electrical heating is applied to the column, 10 m of which has a resistance of ∼112Ω. A centre tap is made and the two halves heated in parallel (28Ω) and a 24 VDC supply provides at most 26 W which alone is not enough for fast ramping of the column temperature. An additional 30 W heating is applied to the aluminium endplates using patch heaters. The response of the column is extremely fast compared to the endplates. During a temperature program the endplates lag by several degrees but the fast response and the direct heating of the column ensure that the desired temperature profile is achieved with minimal error. Column and endplate heating are under PID mark-space control. A typical temperature program consists of a 2 min run-in at 25 °C followed by a linear rise to 175 °C at 30 °C min^{-1}, ending with a 2 min isothermal run-out at 175 °C (Fig. 3). For aircraft and ground-based deployments the column and cage are mounted in an oven enclosure made from 5 mm foamboard and internally insulated with Microtherm thin sheet and Mylar film. At the end of each heating cycle, a fan cools the column back to the starting temperature ready for the next cycle. For MIR balloon flight the column assembly is mounted in a polystyrene housing located underneath the instrument away from solar radiation. This allows the column to be cooled by a fan drawing in external air at ambient temperatures down to −60 °C.

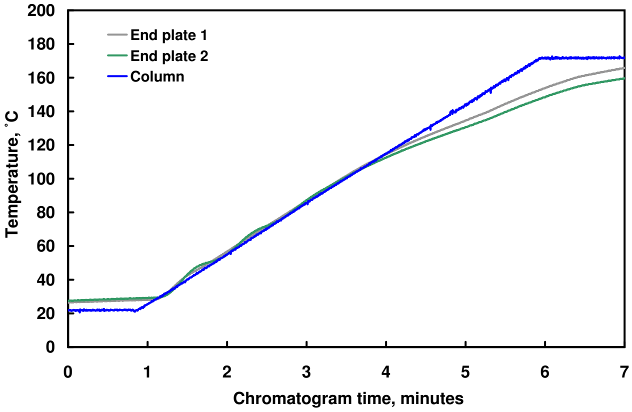

Fig. 3. Performance of the programmed column oven during a linear temperature rise from 20 °C to 175 °C at 30 °C min^{-1}. The three lines show the simultaneous temperatures of the oven end-plates (grey and green) which provide the bulk of the power and of the column itself (blue) which provides additional regulations from direct heating.

Helium pressure controller. To achieve reproducible peak retention times it is necessary to accurately control the helium carrier gas flow, and a novel regulator has been developed for this purpose. A solenoid valve controls the input of helium into a small reservoir through a restrictor formed by a length of 1/32″ OD 0.0035″ ID PEEK tube. The pressure in the reservoir is sensed using absolute pressure sensors and when this falls below a dynamic threshold the valve is opened to admit helium until the upper threshold is reached. This results in a saw-tooth pressure profile. A second reservoir is connected by another length of PEEK capillary tube forming, by analogy, a low pass filter. The pressure in this second, output reservoir is also measured and fed into the PID control. In this way the column head pressure is controlled to within ± 0.2% relative standard deviation (RSD) of the setpoint. The column head pressure is programmable in terms of start/end point pressure and ramp rate. As the column temperature rises, the increase in viscosity of the helium carrier gas results in a decreased flow for a constant column head pressure. To maintain the optimum carrier flow rate (∼0.3 $\mathrm{cm}^3\ \mathrm{min}^{-1}$) the helium column head pressure is ramped. A typical helium pressure program is 127 kPa for the 2 min isothermal run-in followed by a linear rise to 143 kPa at 3 kPa min^{-1}, finishing with a 2 min run-out. The outflow from the pressure controller is passed through an in-house purifier. At the end of the cycle a solenoid valve vents excess helium to lower the pressure back to the starting set point for the next cycle.

Detection system. Target halocarbon molecules pass from the column (via the transfer tubing) into the micro-volume ECD (Agilent Technologies, model G2397-60510) where they are ionised within an electron field formed by ionisation of a nitrogen make-up gas from primary electrons emitted from the ^{63}Ni foil. The detector has a hidden anode design to minimise the need for cleaning and is furnished with a nitrogen anode purge flow in addition to the nitrogen make-up flow. The detector has an internal cell volume of 0.15 cm^3 and is ideally suited to capillary column chromatography. An electrometer maintains a constant current across the cell and the pulse frequency increases when electron-capturing molecules enter the cell. Software control of detector current and offset is achieved by using digitally controlled potentiometers. A 16 bit analogue to digital converter (ADC) "oversamples" the electrometer signal at 20 ms intervals and averages to produce the final 5 Hz output. The detector is coupled to an aluminium heating block with cartridge heater and PT100 temperature sensor. The detector heater is PID controlled to within ± 0.1% RSD of the setpoint. The detector assembly is mounted in a stainless steel vacuum flask for thermal insulation.

The sensitivity of the ECD is temperature dependent. Using a NOAA-ESRL calibration standard containing ∼2 ppt of tetrachloroethene we obtained signal to noise ratios (SNR) of 86, 155, 206 and 203 for ECD temperatures of 200, 225, 250, 275 °C respectively. The highest SNR was typically found at an ECD temperature of 250 °C for the other target halocarbons. We therefore selected a detector operating temperature of 250 °C, which is generally lower than that reported for other instruments (Bassford et al., 1998). At 250 °C the ECD is hot enough to avoid accumulation of contaminants when run continuously for extended periods (months).

Nitrogen pressure controller. Nitrogen is used for the detector anode purge and make-up flow. Precise control of these flows is achieved by a pressure controller similar to that used for controlling the helium carrier head pressure but without the need for a vent valve. The output nitrogen pressure is controlled to within ± 0.1% RSD of the setpoint. The make-up and anode purge flows are typically 5 $\mathrm{cm}^3\ \mathrm{min}^{-1}$ and 0.5 $\mathrm{cm}^3\ \mathrm{min}^{-1}$ respectively. Flow rates can be adjusted by changing the output pressure set point or by changing the length of the PEEK capillary flow restrictors. The nitrogen flow passes through an in-house purifier at the exit of the pressure controller.

Back pressure controller. The detector response is sensitive to changes in atmospheric pressure which can be large during airborne deployments. In addition, changes in atmospheric pressure during ground-based deployment can cause changes in peak retention times. To avoid this, the ECD cell pressure is controlled by using a pressure controller similar to that for the nitrogen flow but controlling the upstream (back) pressure rather than a downstream head pressure. The back pressure is typically 110 kPa and is controlled to within ± 0.2% RSD of the setpoint.

Electronics backplane. Software control is integral in the design of μDirac. The electronic design is modular and consists of a backplane with sockets for nine plug-in boards which are linked peer-to-peer by RS485. Each board has its own PIC microcontroller so that the processing tasks (e.g. flow control, ECD electrometer, column oven ramping) are distributed. The "primary" control board runs the chromatographic method in flash memory and can store data locally on removable memory card (MMC). The control board also handles communication with the PC user interface. For aircraft and ground-based deployments it is convenient to store data on the PC using USB flash memory.

Control. A consistent design aim has been to make all parameters configurable and held either in EEPROM or flash memory. The instrument is either quiescent, where parameters such as gas pressures are maintained or it is operating in program mode. The chromatographic method is written as a text file using a spreadsheet before being compiled and passed to the instrument where it is held in flash memory. The user can configure temperatures, pressures, timings and so on. In addition the user can call for parameters to be recorded in a system file at run time for later analysis (e.g. sample volume). Once the instrument has been deployed, it is possible to remotely view/edit instrument parameters or download a different chromatographic method.

Power supplies. The core GC is designed to operate from 24 VDC for flexibility of deployment. The column and detector ovens use this supply directly. DC/DC converters provide regulated power for solenoid valves at 12 VDC with further regulation to 5 VDC for the electronics. The electrometer requires regulated ± 15 VDC power which is also provided from a DC/DC converter. The thermal desorption system requires a 12 VDC high current supply, provided by a NiMH battery pack and maintained by a trickle charge. The instrument can be run off 100/240 VAC mains or from 24 V batteries.

2.2 Requirements for MIR balloon deployment

The MIR balloon platform has been in development since 1977 by the Centre National d'Etudes Spatiales (CNES, Toulouse, France). It is a hot air balloon of 36 000 to 45 000 m^3 and it is lifted to the stratosphere by helium which exits from the balloon during the first few days of flight. The balloon is heated by radiative fluxes from the sun by daytime and upwelling infrared fluxes during the night which causes the balloon to rise at dawn and descend at sunset, enabling vertical profiles to be measured. The night-time air temperature inside the balloon envelope needs to be at least 15 °C above ambient air to keep a balanced float level and for this reason the envelope is optimized to capture infrared fluxes rising from the earth (about 250 Wm^{-2} available at flight level). The balloon can carry a maximum payload at its hook of ∼50 kg.

This is a technically challenging deployment to deliver scientifically useful measurements at very low atmospheric pressure (5 to 80 hPa) and at very low air temperatures (-20 to -60 °C). The gondola (supplied by CNES) provides protection during launch, thermal insulation, power and communication throughout the 30 day mission. We now describe how each of the technical requirements for the instrument are achieved.

Sampling pump and inlet. The challenge for the pump is to deliver an uncontaminated supply of sample air at high enough pressure to provide flow through the sampling manifold including the narrow adsorbent tube. A commercial diaphragm or metal bellows pump cannot be used due to power, weight and contamination issues. Instead the design is in-house, based on two 100 cm^3 glass laboratory syringes each with a solenoid valve for flow control. The syringes are each driven by a gas actuated cylinder with magnetic/reed switch stroke detection and are operated 180° out of phase (Fig. 4 – left panel). A differential pressure sensor determines when the pump pressure is sufficiently high to be directed into the core GC. The target sample volume is 5 cm^3 at standard temperature and pressure (STP) which can be obtained by about 3 pump cycles at an ambient pressure of 20 hPa. Each syringe is fitted with a 2 m length of inlet tubing below the gondola to allow sampling of uncontaminated air during descent.

Helium and nitrogen gas supply. The GC requires nitrogen, helium and calibration gas for the duration of the MIR balloon flight. We assume a duration of 30 days though MIR balloons have previously flown for over 11 weeks. The nitrogen and helium supplies are held in 1.5 l aluminium/glass fibre composite cylinders, each equipped with a three way filling valve. The cylinders are filled to ∼200 bar with grade 6.0 nitrogen and helium. The helium and pressure controllers in the core GC need an input pressure of 3 to 5 bar absolute and this is delivered by high purity absolute pressure regulators. The sampling pump actuators also need a delivery pressure of 3 to 5 bar which is taken from the output of the helium regulator.

Calibration gas supply. The instrument requires regular calibration during the balloon flight. The standard mode, to be used on all profiles, is for a calibration chromatogram to be run at the start and end of each vertical profile, giving 10 samples between calibrations. To assess the amount of sensitivity drift during a vertical profile, an operating mode is available which alternates between sample and calibration chromatograms. There is also a calibration mode which generates a five point calibration response curve to enable correction for instrument non-linearity effects. Calibration gas is stored in a 75 cm^3 Sulfinert treated cylinder fitted with a stainless steel bellows valve. The cylinder is filled to 68 bar before flight by decanting from a NOAA-ESRL calibration cylinder which is linked to NOAA-ESRL halocarbon standard scales (Hall et al., 2001). The calibration gas is supplied to the core GC at a pressure of ∼2 bar absolute by a high purity absolute pressure regulator.

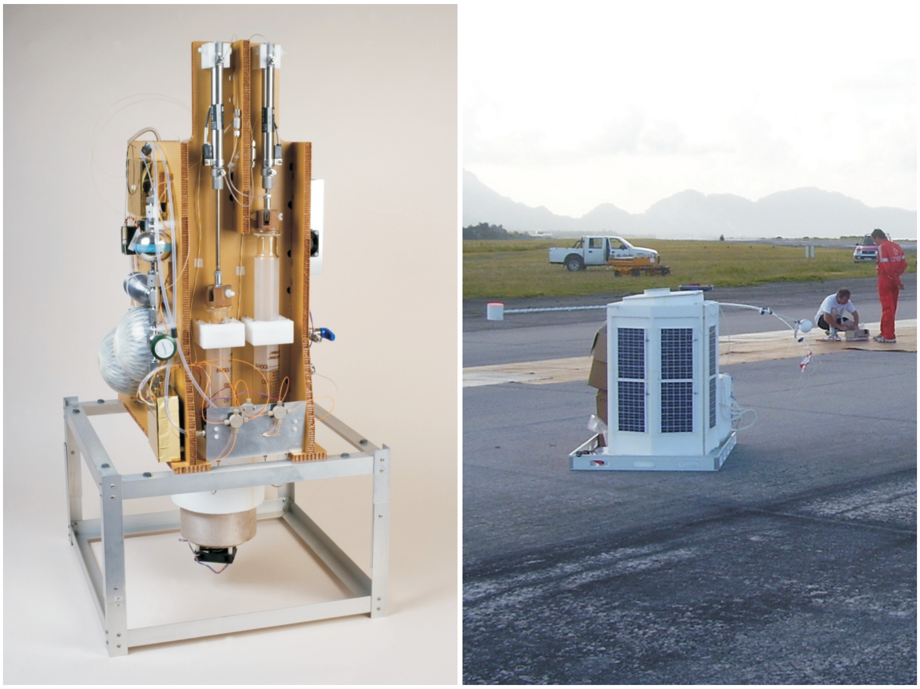

Fig. 4. (left) MIR μDirac armature showing twin syringe sample pump; (right) MIR flight housing on the launch pad in Mahé, Seychelles.

Power and housing. The overall power consumption when active reaches a peak of 50 W and drops to ∼10 W when the instrument is in quiescent mode. When flying, it only measures for a few hours each day when the balloon altitude changes at sunrise and sunset so it can be quiescent for most of the time. The CNES gondola provides power from primary lithium cells together with a nominal 24 V electrical supply from 6 solar panels. During daylight the solar power is configured to heat the detector oven. The core GC, pump and gas supply are all supported on an armature constructed from light weight honeycomb composite sheet (Fig. 4 – left panel). The instrument is housed inside the CNES polystyrene gondola which also contains the lithium battery packs and communications module (Fig. 4 – right panel). The column oven is located in the base of the gondola to assist in rapid cooling of the column at the end of each chromatogram. The overall weight of the MIR instrument (core instrument, pump and gas packs) is ∼11 kg.

Communication. Each balloon profile is initiated by sunrise or sunset and the instrument needs to anticipate these events by one hour. On receiving a “wake-up” command from a CNES payload service board (PSB) the instrument becomes active, temperature and pressure set points stabilise and a calibration run is made. As each run is completed, data are passed to the PSB module for upload to the INMARSAT satellite network. Through commands input in Toulouse, the PSB is able to switch the instrument between 7 different operating modes. The PSB is equipped to turn the instrument on or off. All these features were tested at low temperature and low pressure prior to flight in the CNES stratospheric simulator, with μDirac successfully running (a) overnight at −60 °C and (b) simultaneously at 100 hPa and −60 °C. The full communications between μDirac and the CNES PSB were also tested up to and including upload of data via satellite and download to Toulouse (and the mirror site in the Seychelles).

Attempted MIR long duration balloon flight. On the evening of 17th February 2008, μDirac was launched on a MIR balloon from Mahé International Airport, Seychelles (4.68° S, 55.53° E). The balloon ascended to 38 km and began tracking west across the Indian Ocean towards the East African coast some 1600 km distant. The instrument was programmed to remain in standby mode during the night and to start the first sampling sequence at dawn. However, on the first morning, a serious communication problem developed between the ground control station and the CNES balloon flight control gondola. For several hours CNES personnel attempted to regain communication and control of the balloon but with no success. At the end of this period an automatic timer triggered a cut-down of the balloon (standard safety practice in the event of a major communication failure). The equipment below the balloon descended by parachute and entered the Indian Ocean at 5.80° S, 46.82° E. No recovery attempt was possible at short notice and the instrument was lost. No μDirac sample data were recovered as the communication failure occurred before the end of the first sampling sequence. In addition, no system or calibration data were recovered and so it was not possible to assess technical performance in terms of precision, altitude sensitivity dependence and stability of response curves. There was no immediate flight of the back-up instrument which is being kept in case of a future flight opportunity.

2.3 Requirements for aircraft deployment

μDirac was deployed on the Natural Environment Research Council (NERC) airborne research and survey facility (ARSF) Dornier 228 aircraft for low altitude (<5 km) in the Cape Verde Islands in May/June 2007. This was technically easier than the MIR balloon flight as aircraft power was available, ambient pressure was higher, the thermal environment was less extreme and the required degree of autonomy was lower (typical aircraft flight was 4 h duration).

Sampling pump and inlet. For low altitude operation the sampling pump is located at the exit of the core GC to reduce the risk of sample contamination. This is possible as the required pressure differential across the inlet manifold can easily be obtained by lowering the sample outlet pressure. The pump maintains a sub-ambient reservoir of ∼16 kPa inside a 600 cm^3 canister. By adjusting the pressure in this reservoir the sample flow rate through the core GC can be set (typically between 5 and 20 $\mathrm{cm}^3\,\mathrm{min}^{-1}$). The sample inlet line of the core GC is connected to a ∼10 m of PFA tubing flushed at a flow rate of ∼1 $\mathrm{l\,min}^{-1}$ using a miniature rotary vane pump. The sample flow passing into the core GC is dried using a dessicant Nafion membrane drier. Laboratory tests which passed calibration air through the Nafion tube showed no loss of target halocarbons and also blank tests (using purified nitrogen) showed no presence of contaminants co-eluting with target peaks.

Helium, nitrogen and calibration gas supply. The core GC requires sufficient helium, nitrogen and calibration gas for several days of operation as refilling the gas cylinders is difficult on an aircraft. For the Dornier deployment, a gas pack housing made from honeycomb composite sheet secures the cylinders. Grade 6.0 helium and nitrogen are stored at up to 120 bar in aluminium cylinders of 300 cm^3 and 1200 cm^3 volume respectively. The calibration gas system is identical to that for the MIR version except that the cylinder is larger (150 cm^3). A full gas pack can run the instrument for ∼10 days of continuous operation.

Power, housing and computer. The instrument can run from 240 VAC aircraft power. A regulated power supply is used to supply 24 VDC power (maximum ∼5 amps) to the core GC. To provide unbroken power to μDirac during engine startup and shutdown a simple uninterruptible power supply (UPS) is used, made from two 12 V battery packs in series. The need for a strong instrument housing on the Dornier is paramount over weight considerations, therefore the core GC and gas pack are mounted on a slide-out shelf inside a steel 19″ 9U rack enclosure. The enclosure is fitted with fans to remove excess heat from the instrument. In addition, air is provided to the column fan at ∼5 °C below ambient air temperature by a Peltier heat pump. This ventilation does not impair the thermal stability of the ECD and column oven which are well insulated. A single board PC is used to start the instrument before flight and to store data in-flight. This is low power, has in-built UPS protection and solid state disk drives rather than mechanical drives (which can fail at reduced ambient pressure). The PC also runs the control interface and instrument data are stored on USB flash memory.

2.4 Requirements for ground-based deployment

Here we describe the technical requirements needed to support the core GC for long ground-based or ship deployments where the instrument will be unattended for long periods. The requirements are similar to those required on aircraft deployment but with a longer sample inlet, support gases for several months and a robust power scheme to handle power outages.

Sampling pump and inlet. The PFA inlet tubing can be up to 80 m long. Ingress of rain at the top of the inlet is avoided by an upturned glass funnel plugged at its inlet by glass wool to exclude insects and large particles. The inlet is flushed by a pump located downstream of the instrument inlet tee. A counter flow Nafion membrane drier is used to dry the sample flow passing into the core GC using the detector exhaust gas as the drying flow. Laboratory tests using humidified air showed the drier could lower the relative humidity from 95% at the input to 3% at the output with a counter flow of 5 $\mathrm{cm}^3\,\mathrm{min}^{-1}$.

Helium, nitrogen and calibration gas supply. The core GC requires sufficient helium, nitrogen (6.0 grade) and calibration gas for several months unattended operation. For the helium and nitrogen gases, small commercially available 10 l size cylinders with high purity single stage pressure regulators are used. With a fill pressure of 200 bar the nitrogen and helium last for 9 and 45 months continuous operation respectively. The calibration gas system is identical to that for the MIR balloon but with a larger Sulfinert cylinder (500 cm^3), giving a capacity of 34 l of calibration gas (sufficient for 4 months typical operation). For longer deployments a NOAA-ERSL standard contained in a 34 l stainless steel “Essex” cylinder is used directly.

Power, housing and computer. Where 100/240 VAC mains power is available μDirac uses a regulated 24 VDC power supply backed up by a UPS. In the absence of mains power the instrument can be operated outdoors (e.g. on the forest floor) by employing pairs of 12 V battery packs in series (e.g. NiMH packs or 12 V lead acid car batteries). In this way the instrument can run for hours to days depending on battery capacity. The instrument is housed in a lightweight (4 kg) plastic 19″ 8U rack enclosure which can easily be carried between sites. Cooled air is provided to the column fan and adsorbent tube using a Peltier heat pump. A low power, single board PC identical to that used for aircraft deployment is used to run the user interface and data collection software.

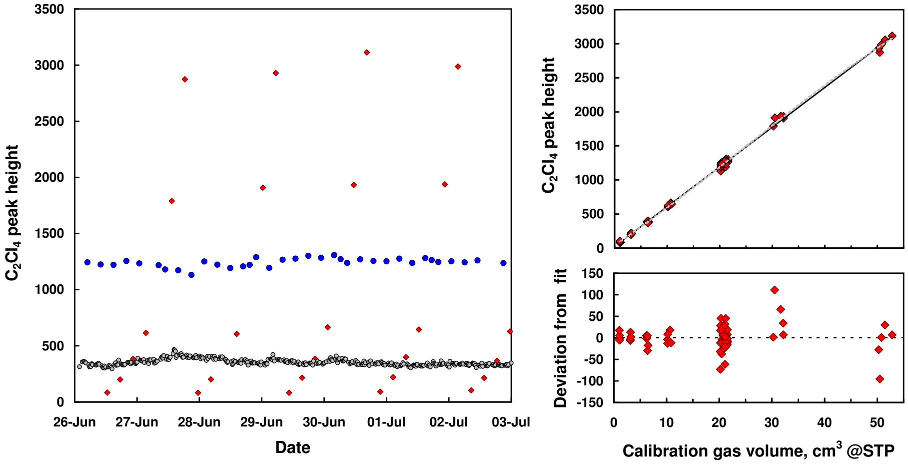

Fig. 5. (left) Typical μDirac calibration / sampling sequence showing raw peak height data for tetrachloroethene (from 26th June to 3rd July 2009, during remote operation at Bukit Atur, Malaysia). Sample peak heights are shown as grey circles. Precision calibrations (blue circles) are used to derive measurement precision and to enable correction to sensitivity drift. The response calibrations (red diamonds) are used to make corrections for non-linearity. (right) The response calibration peak heights plotted against volume of calibration gas. The solid black line shows the linear fit and the dashed grey line is a 3rd order polynomial fit. The lower panel shows the deviations of the individual calibrations from the linear fit and more clearly shows any departure from linear behaviour, the dashed black line in this panel is a linear fit through the deviations. Note that we anyway use the 3rd order polynomial fit to correct the samples for non-linearity effects.

A flat panel monitor, keyboard and mouse are added, though these are removed for deployment outdoors.

3 Instrument performance

Here we describe the performance of μDirac based on laboratory tests and on results of recent field deployments. High quality geophysical data is possible only after detailed attention to instrument calibration, accuracy, precision, peak separation and sensitivity. We now describe each of these performance aspects in turn.

3.1 Calibration

Absolute calibrations are determined by reference to a NOAA-ESRL calibration gas standard. This is a pressurised, humdified sample of air from Niwot Ridge (CO, USA) held in a 34 l stainless steel electropolished "Essex" cylinder (filled to 60 bar in December 2005). Niwot Ridge is a site representative of remote continental background air. The standard was spiked with a few ppt of CH_3I, $CHBr_3$ and CH_2Br_2 and compared to NOAA-ESRL working standards using GC-ECD and GC-MS techniques enabling accurate ppt (dry air mole fraction) determination for 21 halocarbons. Typical uncertainty in the calibration gas is ± 0.5 to ± 2% (2 s.d.) for the CFCs and other long-lived halocarbons and ± 5 to ± 20% for the shorter-lived halocarbons (B. D. Hall, personal communication, 2010). NOAA-ESRL recommend re-analysis of the calibration cylinder to assess drift every 3 years or when the cylinder pressure drops to 20 bar.

In Cape Verde (May–June 2007), calibration chromatograms of the same volume as the samples (~20 cm^3) were run after typically every 6 sample chromatograms (the calibration frequency can be changed in the method file). A blank chromatogram, generated by sampling helium purge gas, was also run just before every calibration as a check on system impurities and desorption efficiency. The instrument method now includes calibration response curves (several calibrations covering a range of volumes) which enable the tracking of small changes in detector non-linearity (Fig. 5). Some compounds show a near linear instrument response (e.g. C_2Cl_4) whilst others show some degree of non-linearity (Fig. 6). We correct for non-linearity using response curves which are continually collected autonomously over a few days.

3.2 Accuracy and precision

Taking into account the various uncertainties such as those associated with preparation of the standard, drift of standard with time, changes due to transfer of standard gas to the on-board cylinder, we estimate that an accuracy of ± 2 to ± 5% (2 s.d.) can be achieved for the long-lived halocarbons and ± 10 to ± 25% for the shorter-lived compounds. The estimated uncertainties of the measurements for individual halocarbons are given in Table 1. These errors are reviewed as more knowledge is acquired of the various uncertainties (e.g. standard drift with time).

The measurement precision cannot be estimated directly in the samples. One way to assess this is by repeating the measurement of the gas standard several times consecutively

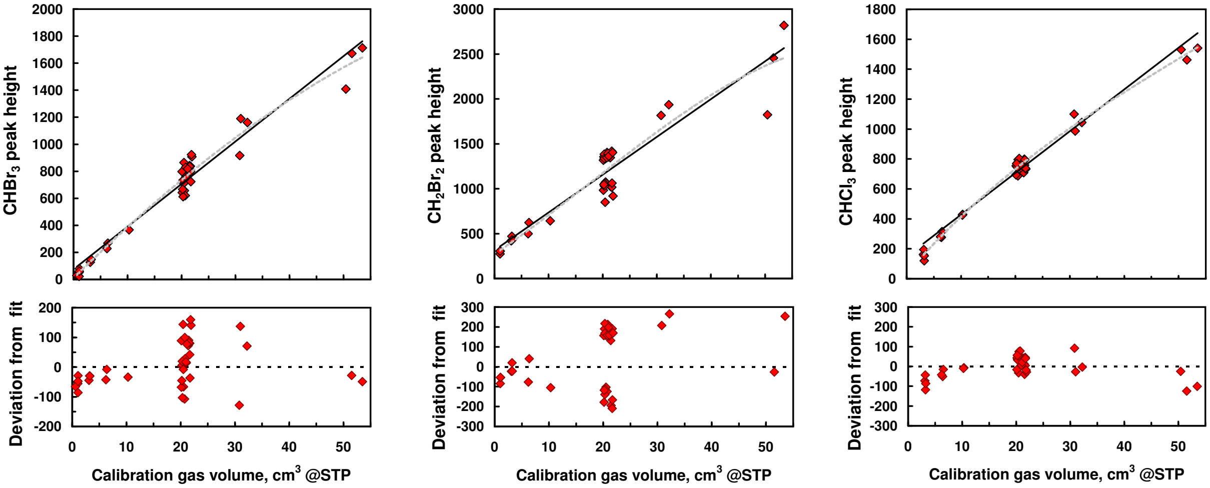

Fig. 6. Typical μDirac calibration response curves showing raw peak height versus calibration volume for bromoform (left), dibromomethane (centre) and chloroform (right). Individual calibrations are shown as red diamonds, the solid black line is the linear regression and the dashed grey line is a 3rd order polynomial (used for the non-linearity correction). To highlight any departure from linearity the lower panel for each compound shows the standard deviation from the linear fit of the calibration points and the dotted black line in the lower panels is the linear fit through the deviations. The measurements were made in 2009 (26th June to 3rd July) during remote operation at Bukit Atur, Malaysia.

and calculating the RSD of the peak heights for each target compound. Using this approach in the laboratory we obtain RSDs for target compounds ranging from ± 0.9% (C_2Cl_4) to ± 8.5% ($CHCl_3$), based on a 20 cm^3 calibration air volume (Fig. 7 – upper panel). To quantify measurement precision in the field, we look at the real-time calibration chromatograms run typically after every six samples in the Cape Verde ground-based campaign (Fig. 7 – lower panel). The field precisions for 20 cm^3 calibration air vary from ± 1.1% for CCl_4 up to ± 9.3% for CH_3I and are given in Table 1. In-flight (Dornier) RSD measurement precision ranges from ± 1.9% for CCl_4 up to ± 20.2% for CH_3I. The laboratory precision tests were made under more stable thermal conditions than those from the field and hence they are better. Environmental conditions in the field are not usually optimal and so the laboratory performance is not always attained. The laboratory based estimates presented here thus represent the best achievable performance and they are approached when instruments are run for extended periods in stable surroundings. μDirac has been designed so that its operating conditions are as stable as possible in order to minimise any additional error contributions.

3.3 Separation and co-elution

Unlike a mass spectrometer, the ECD is not capable of differentiating between two or more peaks which elute at the same time from the column. For this reason, optimum separation of the target compounds (and from other unknown compounds) is very important. Fortunately, the ECD is selective and in the case of atmospheric samples it mainly responds to halogenated and oxygenated compounds and shows little response to hydrocarbons for instance. The 10 m column used on μDirac allows good separation of target compounds in samples with overall analysis times as short as 10 min (Fig. 8), but there are some co-elution issues. During instrument development we introduced individual target halocarbons by preparing crude static dilutions (typically 50 to 100 ppt in a nitrogen balance) from single analyte solutions, sourced commercially. This provided retention time information for target compounds. We then extended this work by introducing compounds which (from the literature) may be found in atmospheric samples, even at sub-ppt levels. We identified a co-elution issue with CH_2Br_2 and $CHBrCl_2$ as this appears just before CH_2Br_2 in our chromatograms but there is no valley between the peaks. Measurements of CH_2Br_2 as $CHBrCl_2$ reported in the literature indicate that CH_2Br_2 is usually present at higher mixing ratios than $CHBrCl_2$ (between 3×and 10×higher) at least for marine air (O'Brien et al., 2009). Other compounds which we have investigated as possible candidates for co-elution with our target compounds are 1,1-dichloroethene, bromoethane, iodoethane, *n*-iodopropane, chloroiodomethane, 2-iodopropane, 2-iodobutane, 1-iodobutane, 1,1,1,2-tetrachloroethane, 1-iodopentane (Fig. 9). There are also some possible co-elution issues with alkylnitrates which can be present at high concentrations in biomass burning plumes. On-going work has identified likely compounds (of biomass burning origin) which we will subsequently try to investigate further using the μDirac column. Also, we are using longer columns to address co-elution issues and are investigating different column types.

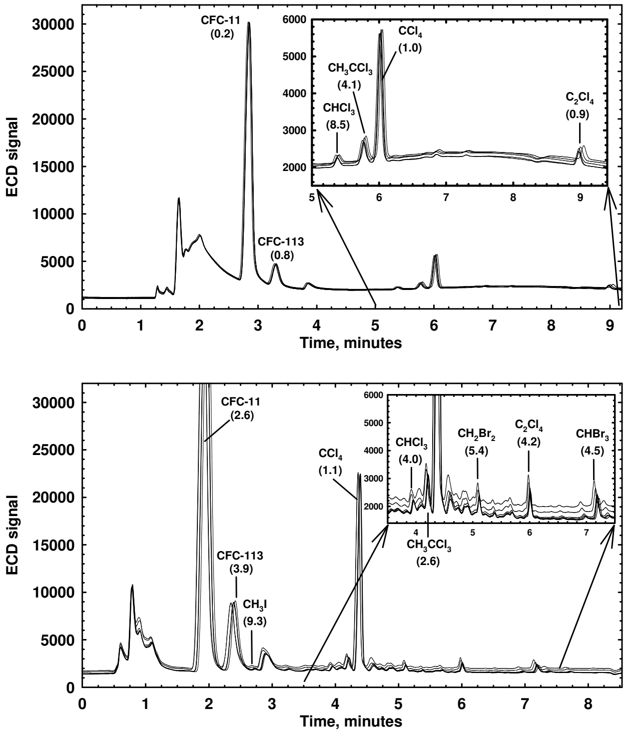

Fig. 7. Overlaid chromatograms of calibration air during operation in the laboratory (upper panel) and in Cape Verde in June 2007 (lower panel). The precision of the peak heights (RSD,%) are shown in parentheses, each chromatogram is generated from a 20 cm^3 volume of Niwot Ridge air (NOAA-ESRL) spiked with CH_3I, CH_2Br_2 and $CHBr_3$.

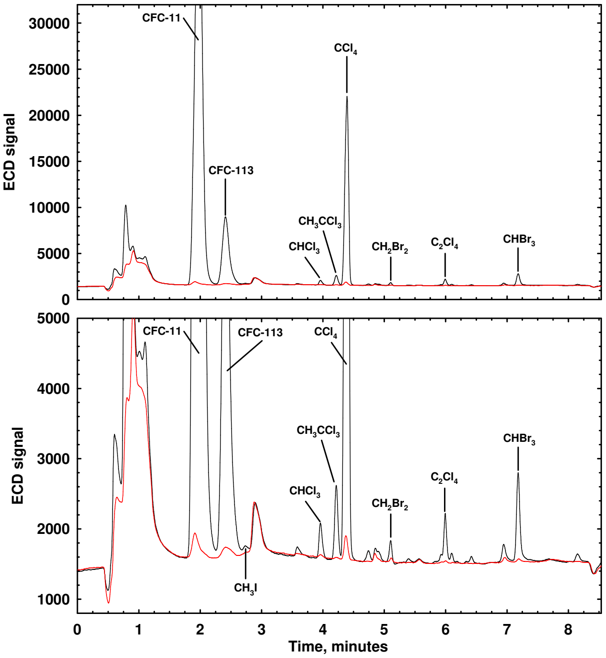

Fig. 8. (upper panel) Sample (black trace) and blank (red trace) chromatograms from the Cape Verde campaign in June 2007. (lower panel) Same chromatograms as upper panel but zoomed in to more closely show the baseline, including smaller target peaks and blank levels.

Some peak broadening is evident in μDirac chromatograms despite the use of a narrow bore capillary column. When desorbing it is important that the carrier flow is close to the optimum for the column (0.3 cm^3 min^{-1}). However, this is below the optimum flow rate for desorption and results in non-instantaneous injection onto the column. We have tried using a smaller bore adsorption tube (0.25 mm ID) which would have a lower optimum flow for desorption. However this proved too small for the mesh size of adsorbent used and caused a blockage. Peak broadening in our chromatograms is also partly due to the dead volume in the ECD and low make-up gas flow used, which particularly affects the front of the chromatogram around CFC-11 and CFC-113.

3.4 Sensitivity

The instrument has been optimised for high sensitivity. The micro-volume ECD is arguably the most sensitive ECD available commercially and has the lowest internal cell volume. This allows capillary columns to be used with low make-up gas flow (the flushing time of the cell is shorter than a conventional ECD). The nitrogen make-up flow is typically 5 cm^3 min^{-1} in order to further improve sensitivity. The electrometer and ADC have both been designed to minimise noise interference with the result that detector noise approaches the quantisation step of the ADC. Although we have optimised the method for a sample volume of 20 cm^3 it is also possible to increase sample volume and thus improve detection limit slightly. However, for larger sample volumes there is increased likelihood of breakthrough on the adsorbent bed and volumes much larger than 50 cm^3 may require a larger adsorbent tube and possibly an increase in the scale of the system (e.g. larger bore column).

A common way to assess sensitivity is by calculating the limit of detection from the SNR. We calculate the SNR as the ratio between the peak height of interest and the root mean square (RMS) of the baseline noise. For example, the smallest known peak in Fig. 7 (lower panel) is CH_3I with a peak height of 128 and the RMS of the baseline noise is 2.05 giving a SNR of 62. The concentration of CH_3I in the calibration standard is 3.4 ppt, resulting in a detection limit of 0.5 ppt for a sample volume of 20 cm^3 (detection limit defined here for SNR = 10). The detection limits for the halocarbons measured by μDirac are given in Table 1 assuming that a sample of 20 cm^3 is collected.

An additional quantity used in assessing sensitivity is the limit of quantification, defined as the smallest detectable amount of a compound which is statistically larger than zero. The ideal way to test for this is to introduce known

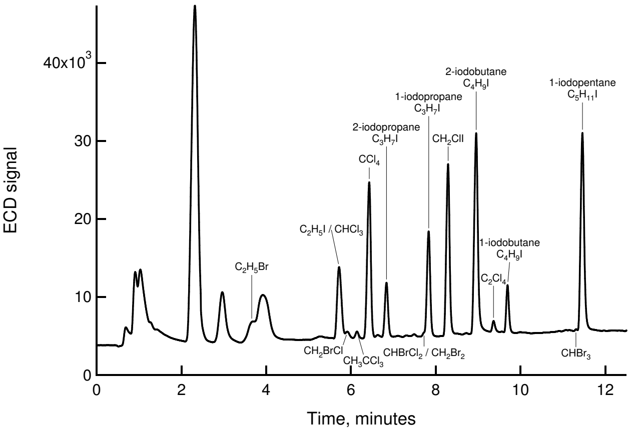

Fig. 9. Chromatogram of a laboratory air sample from μDirac after spiking the laboratory air with traces of nine different halocarbons: bromoethane (C_2H_5Br), iodoethane (C_2H_5I), 1-iodopropane (C_3H_7I), chloroiodomethane (CH_2ClI), 2-iodopropane (C_3H_7I), 2-iodobutane (C_4H_9I), 1-iodobutane (C_4H_9I), 1-iodopentane ($C_5H_{11}I$). To enable clear retention time identification the halocarbons were introduced individually and a laboratory air chromatogram was made before introducing the next compound. This was purely a qualitative exercise; however our latest NOAA-ESRL standards do include chloroiodomethane on a provisional scale (estimated accuracy ± 10 to ± 20%, 2 s.d).

amounts of each halocarbon at a concentration just above the limit of detection. Then by measuring the RSD of repeat chromatograms we can deduce if the measurement precision for peaks with very low SNR is the same as that for high SNR peaks. We have looked at this for C_2Cl_4 (using ground-based data) and found an RSD of ± 2% for samples of 2 ppt (SNR 330). The precision degrades to ± 5% for samples of 0.3 to 0.7 ppt (SNR 50 to 100) and degrades to ± 11% for samples of 0.1 ppt (SNR 10). For CH_3I which is the smallest target peak in our chromatograms, the RSD is typically ± 4% for samples of 2.5 ppt (SNR 15) but the RSD degrades to around ± 28% for samples of 0.5 to 1.0 ppt (SNR ~10). The reason for choosing SNR = 10 to define the detection limit is that the integration software used to detect and measure peaks does not work for SNR lower than 10. Conversely, though, this means that μDirac can measure compounds at their detection limits with reasonable precision.

4 Results and Discussion

μDirac has already participated in several deployments: ground-based, aircraft and balloon campaigns. In this section we demonstrate the field capability of the instrument by presenting results from an aircraft campaign and a ground-based deployment.

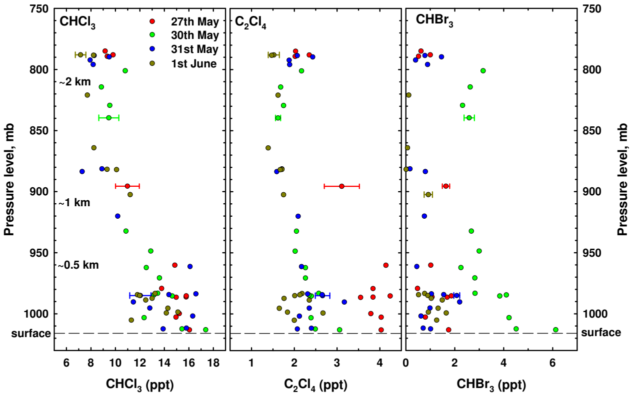

Fig. 10. Vertical profiles of $CHCl_3$, C_2Cl_4 and $CHBr_3$ mixing ratios (dry air mole fraction), measured near the Cape Verde Islands by μDirac aboard the NERC-ARSF Dornier 228 aircraft in May/June 2007.

4.1 Cape Verde Dornier flights

The NERC-ARSF Dornier 228 aircraft was stationed on São Vicente Island, Cape Verde (São Pedro Airport, 16.83°N, 25.06°W) between 25th May and 1st June 2007 as part of the Reactive Halogens in the Marine Boundary Layer (RHaMBLe) campaign. The aircraft carried instrumentation from the Universities of York, Leeds and Birmingham in addition to μDirac. Twelve short, local survey flights (3 per day) were performed in the vicinity of the Cape Verde Atmospheric Observatory and an additional three longer "rendezvous" flights were made to the NERC vessel RRS Discovery, which was also involved in the RHaMBLe campaign. Vertical profiles of $CHCl_3$, C_2Cl_4, and $CHBr_3$ from μDirac indicate that the aircraft predominantly flew in background air remote from anthropogenic influence (Fig. 10). The greater variability of all three gases in the lower boundary layer is consistent with the ground-based observations which started at this time (O'Brien et al., 2009), with the concentrations of $CHCl_3$ and C_2Cl_4 being elevated when the air had previously passed over western Europe and high variability in the $CHBr_3$ concentrations.

4.2 Operation in Malaysian Borneo

From April to July 2008, the NERC funded Oxidant and Particle Photochemical Processes (OP3) project studied forest emissions in Sabah, Malaysian Borneo. The ground-based part of the campaign was based at the Global Atmospheric Watch (GAW) station at Bukit Atur, located in a tropical lowland dipterocarp forest (Danum Valley, 5°N, 118°E). Two μDirac instruments were deployed, one was based permanently at the GAW station and the other was used to make exploratory measurements in the forest and at the coast. Halocarbon measurements were also made at the GAW station by a GC-MS instrument from the University of East Anglia.

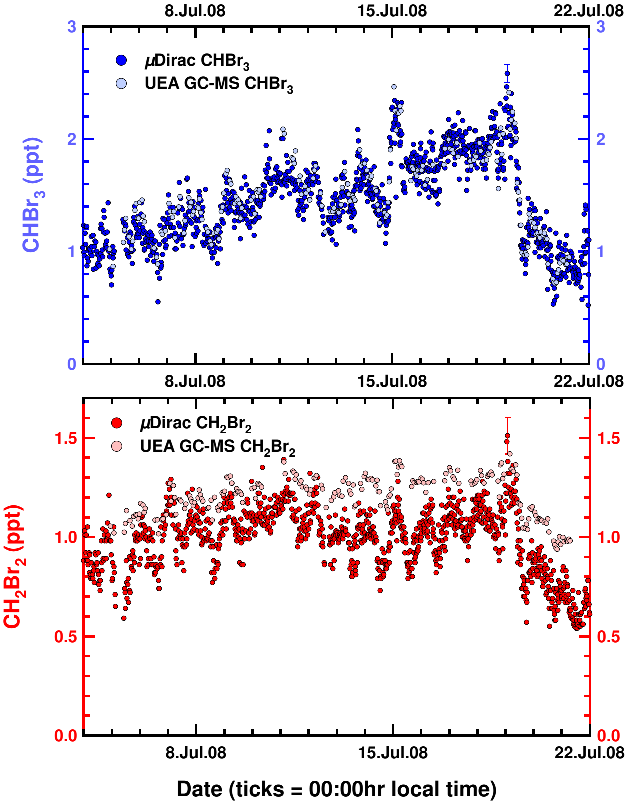

Fig. 11. $CHBr_3$ and CH_2Br_2 mixing ratios (dry air mole fraction) measured at the Bukit Atur GAW station in Danum Valley, Borneo in June/July 2008. The dark symbols are measurements made by μDirac and the light symbols are measurements made by the UEA GC-MS. Both instruments used the same measurement tower with inlets which were 18 m apart in height. Note that the CH_2Br_2 peak in μDirac chromatograms is not resolved from the $CHBrCl_2$peak (we report the combined peak as CH_2Br_2). The estimated 1 s.d. precisions are: $CHBr_3$ – μDirac ± 3% and GC-MS ± 5%; CH_2Br_2 – μDirac ± 6% and GC-MS ± 5%.

This was an Agilent 6890/5973N operating in negative ion, chemical ionisation mode (NICI) with CH_4 as reagent gas. The GC column was a 105 m long (0.32 mm ID) RTX-502.2 with a 1.8 µm film thickness, temperature ramped from 35 °C to 235 °C. One litre air samples were processed on a Markes Unity thermal desorption unit. The UEA halocarbon measurements were referenced to the NOAA-ESRL (2003) calibration scale. Further details can be found in Worton et al. (2008). The two GAW based instruments (μDirac + UEA GC-MS) were sampling almost identically with just an 18m difference in the inlet height.

Both instruments reported observations of $CHBr_3$ and CH_2Br_2 between 4th and 21st July 2008 (Fig. 11). For $CHBr_3$ there is an excellent agreement in both the absolute mixing ratios and the trend. For CH_2Br_2 the μDirac mixing ratios are lower than those of UEA although the trend in the two data sets is similar. Both instruments use NOAA-ESRL calibration scales but it is still reassuring to see such a high level of agreement. The CH_2Br_2 peak in μDirac chromatograms is not resolved from the peak resulting from any $CHBrCl_2$present in samples, therefore we should regard the μDirac CH_2Br_2 measurements as CH_2Br_2+ $CHBrCl_2$. For this 18 day period of forest measurements the average levels of CH_2Br_2 and $CHBrCl_2$ were 1.20 and 0.25 ppt respectively, as measured by the UEA instrument. Based on this, we would expect the μDirac combined CH_2Br_2/$HBrCl_2$ peak to be 83% due to CH_2Br_2 and 17% due to $CHBrCl_2$ (assuming the same ECD sensitivity for both molecules). The average μDirac combined CH_2Br_2 + $CHBrCl_2$ peak was 0.99 ppt, of which an estimated 0.82 ppt could be attributed to CH_2Br_2 (and 0.17 ppt as $CHBrCl_2$), an under estimation of 32% relative to the UEA data. It is a little surprising that the μDirac CH_2Br_2 levels are lower than those of UEA when we expected them to be higher due to the coelution issue. Work is on-going to find the cause of this difference and it is helpful that the μDirac calibration gas was measured by the UEA GC-MS instrument during the campaign. It is possible that there were changes in the μDirac calibration gas when decanted into the portable Sulfinert cylinder large enough to explain this ∼0.5 ppt difference. Across the global science community there are differences in the calibration scales of many shorter-lived halocarbons. An inter-laboratory calibration comparison experiment is taking place in the UK (led by York University) with the aim of reconciling some of these differences for UK measurement groups.

The two ground-based μDirac instruments remained in Sabah after the end of the OP3 field campaign, one instrument remained at the Bukit Atur GAW station and the other was sited at the coast near Tawau (4.22° N, 118.00° E). This dual instrument deployment is the first step in a larger scale project to generate a long time series of halocarbon (and later hydrocarbon) measurements from several coastal sites in the west Pacific.

5 Summary

A new lightweight micro-GC is described. It uses Carboxen™ adsorbents for sampling, a temperature and flow programmable column and a micro-volume ECD. A central feature is on-board (autonomous), precise control of all aspects of the instrument. Designed for use on a long duration balloon, it is lightweight (11 kg without batteries), has low power consumption and can run autonomously for long periods. Unfortunately, it could not prove itself on the long duration balloon due to a balloon failure. However, the novel design needed for the long duration deployment has resulted in a versatile instrument capable of running reliably at the ground for months at a time. The calibration procedure allows any changes in linearity of response to be monitored as well as changes in sensitivity, giving increased confidence in the quality of the measurements. Comparison with the UEA

GC-MS instrument at Bukit Atur shows excellent agreement for $CHBr_3$ and reasonable agreement for CH_2Br_2 given the current state-of-the-art. The reliability of the instrument for continuous operation has been demonstrated in Malaysian Borneo since September 2008, with near-continuous operation from November 2008 until present.

Acknowledgements. We thank Peter Simmonds for valuable advice and guidance, particularly in selecting suitable Carboxen™ adsorbents. We are grateful to CNES (Philippe = Cocquerez, Jean-Marc Nicot and colleagues) for development and testing assistance during the MIR μDirac development phase and for operational activities. We thank Selvan Pillay and staff at Seychelles National Meteorological Services for hosting the MIR campaign. We thank Jean-Pierre Pommereau and Anne Garnier for organizational support on the Seychelles campaign. For testing and development phases prior to the Cape Verde and Borneo deployments we thank Cambridge Botanical Gardens for allowing us to test the instrument in high humidity (tropical) conditions (John Parker, Rob Brett). We thank Bruno Faria and colleagues at the Instituto de Nacional de Meteorologie e Geofisica (INMG) for their assistance at Cape Verde. We thank Carl Joseph, David Davies and colleagues at NERC-ARSF and Ally Lewis (University of York) for his assistance in the campaign. We thank the University of Lancaster, Royal Society (SEARRP), Danum Valley Field Centre and Malaysian Meteorological Department for their assistance with the measurements in Borneo. Finally, we are grateful for the financial support for (i) the instrument development and the MIR deployment provided by NERC (projects NE/C511248/1 and NE/D008085/1) and by the EC (SCOUT-O3 – 505390-GOCE-CF2004); and (ii) the aircraft and ground-based deployments by NERC (SOLAS-RHaMBLe, AMMA-UK and OP3 NE/D002117/1 campaigns and NE/F020341/1 project). L. O'Brien thanks NERC for her studentship and J. A. Pyle thanks NERC-NCAS for their support. N. R. P. Harris acknowledges the support of a NERC Advanced Research Fellowship.

Edited by: H. Schlager

References

Bassford, M. R., Simmonds, P. G., and Nickless, G.: An Automated System for Near-Real-Time Monitoring of Trace Atmospheric Halocarbons, Anal. Chem., 70(5), 958–965, doi:10.1021/ac970861z, 1998.

Blake, N. J., Blake, D. R., Simpson, I. J., Lopez, J. P., Johnston, N. A. C., Swanson, A. L., Katzenstein, A. S., Meinardi, S., Sive, B. C., Colman, J. J., Atlas, E., Flocke, F., Vay, S. A., Avery, M. A., and Rowland, F. S., Large-scale Latitudinal and Vertical Distributions of NMHCs and Selected Halocarbons in the Troposphere over the Pacific Ocean during the March–April 1999 Pacific Exploratory Mission (PEM-Tropics B), J. Geophys. Res., 106(D23), 32627–32644, 2001.

Butler, J. H., King, D. B., Lobert, J. M., Montzka, S. A., Yvon-Lewis, S. A., Hall, B. D., Warwick, N. J., Mondeel, D. J., Aydin, M., and Elkins, J. W.: Oceanic distributions and emissions of short-lived halocarbons, Global Biogeochem. Cycles., 21, GB1023, doi:10.1029/2006GB002732, 2007.

Class, Th., Kohnle, R., and Ballschmiter K.: Chemistry of organic traces in air VII: Bromo- and bromochloromethanes in air over the Atlantic Ocean, Chemosphere, 15, 4, 429–436, 1986.

Colman, J. J., Swanson, A. L., Meinardi, S., Sive, B. C., Blake, D. R., and Rowland, F. S.: Description of the Analysis of a Wide Range of Volatile Organic Compounds in Whole Air Samples Collected during PEM-Tropics A and B, Anal. Chem., 73, 3723–3731, 2001.

Danis, F., Harris, N. R. P., Taylor, W. H., McIntyre, J. D., Simmonds, P. G., and Pyle, J. A.: DESCARTES: A novel lightweight balloon-borne instrument for measurement of Halocarbons, Review of Scientific Instruments, 70, 271–280, 2000.

Hall, B. D., Elkins, J. W., Butler, J. H., Montzka, S. A., Thompson, T. M., Del Negro, L., Dutton, G. S., Hurst, D. F., King, D. B., Kline, E. S., Lock, L., Mactaggart, D., Mondeel, D., Moore, F. L., Nance, J. D., Ray, E. A., and Romashkin, P. A.: Climate Monitoring and Diagnostics Laboratory Summary Report No. 25, 1998–1999, edited by: Schnell, R. C., King, D. B., and Rosson, R. M., U.S. Department of Commerce, 154 pp., 2001.

Lovelock, J. E. and Lipsky S. R.: Electron Affinity Spectroscopy – A New Method for the Identification of Functional Groups in Chemical Compounds Separated by Gas Chromatography, J. Am. Chem. Soc., 82(2), 431–433, 1960.

Lovelock, J. E.: Atmospheric Fluorine Compounds as Indicators of Air Movements, Nature, 230, 379, 1971.

Lovelock, J. E., Maggs, R. J., and Wade, R. J.: Halogenated Hydrocarbons in and over the Atlantic, Nature, 241, 194–196, 1973.

Miller, B. R., Weiss, R. F., Salameh, P. K., Tanhua, T., Greally, B. R., Mühle, J., and Simmonds, P. G.: Medusa: A Sample Preconcentration and GC/MS Detector System for in Situ Measurements of Atmospheric Trace Halocarbons, Hydrocarbons, and Sulfur Compounds, Anal. Chem., 80, 1536–1545, doi:10.1021/ac702084k, 2008.

Montzka, S. A., Butler, J. H., Elkins, J. W., Thompson, T. M., Clarke, A. D., and Lock, L. T.: Present and future trends in the atmospheric burden of ozone-depleting halogens, Nature, 398, 690–694, 1999.

Morris, P. J. T. and Ettre, L. S., The Saga of the Electron Capture Detector, LC/GC-Europe, 20, 473–479, 2007.

O'Brien, L. M., Harris, N. R. P., Robinson, A. D., Gostlow, B., Warwick, N., Yang, X., and Pyle, J. A.: Bromocarbons in the tropical marine boundary layer at the Cape Verde Observatory - measurements and modelling, Atmos. Chem. Phys. Discuss., 9, 4335–4379, 2009, http://www.atmos-chem-phys-discuss.net/9/4335/2009/.

Penkett, S. A., Jones, B. M. R., Rycroft, M. J., and Simmons, D. A.: An interhemispheric comparison of the concentrations of bromine compounds in the atmosphere, Nature, 318, 550–553, doi:10.1038/318550a0, 1985.

Pommereau, J.-P. and Hauchecorne, A.: A new atmospheric vehicle: The Infra-Red Montgolfier, in Scientific Ballooning, pp. 55–58, Pergamon, New York, 1979.

Pommereau, J.-P., Garnier, A., Knudsen, B. M., Letrenne, G., Durand, M., Nunes-Pinharanda, M., Denis, L., Vial, F., Hertzog, A., and Cairo, F., Accuracy of analyzed stratospheric temperatures in the winter Arctic vortex from infrared Montgolfier long-duration balloon flights 1. Measurements, J. Geophys. Res., 107, 8260, doi:10.1029/2001JD001379, 2002.

Prinn, R. G., Weiss, R. F., Fraser, P. J., Simmonds, P. G., Cunnold,

D. M., Alyea, F. N., O'Doherty, S., Salameh, P., Miller, B. R., Huang, J., Wang, R. H. J., Hartley, D. E., Harth, C., Steele, L. P., Sturrock, G., Midgley, P. M., and McCulloch, A. J., A history of chemically and radiatively important gases in air deduced from ALE/GAGE/AGAGE, J. Geophys. Res., 105(D14), 17751–17792, 2000.

Proffitt, M. H., Margitan, J. J., Kelly, K. K., Lowenstein, M., Podolske, J. R., and Chan, K.: Ozone loss in the Arctic polar vortex inferred from high-altitude aircraft measurements, Nature, 347, 31–36, 1990.

Proffitt, M. H., Aikin, K., Margitan, J. J., Lowenstein, M., Podolske, J. R., Weaver, A., Chan, K. R., Fast, H., and Elkins, J. W.: Ozone loss inside the northern polar vortex during the 1991–1992 winter, Science, 261, 1150–1154, 1993.

Ray, E. A., Moore, F. L., Elkins, J. W., Dutton, G. S., Fahey, D. W., Vömel, H., Oltmans, S. J., and Rosenlof, K. H., Transport into the Northern Hemisphere lowermost stratosphere revealed by in situ tracer measurements, J. Geophys. Res., 104, 26565–26580, 1999.

Ray, E. A., Moore, F. L., Elkins, J. W., Hurst, D. F., Romashkin, P. A., Dutton, G. S., and Fahey, D. W.: Descent and mixing in the 1999–2000 northern polar vortex inferred from in situ tracer measurements, J. Geophys. Res., 107(D20), 8285, doi:10.1029/2001JD000961, 2002.

Robinson, A. D., McIntyre, J., Harris, N. R. P., Pyle, J. A., Simmonds, P. G., and Danis, F.: A lightweight balloon-borne gas chromatograph for in-situ measurements of atmospheric halocarbons, Rev. Sci. Instru., 71, 4553–4560, 2000.

Robinson, A. D., Millard, G. A., Danis, F., Guirlet, M., Harris, N. R. P., Lee, A. M., McIntyre, J. D., Pyle, J. A., Arvelius, J., Dagnesjo, S., Kirkwood, S., Nilsson, H., Toohey, D. W., Deshler, T., Goutail, F., Pommereau, J.-P., Elkins, J. W., Moore, F., Ray, E., Schmidt, U., Engel, A., and Müller, M.: Ozone loss derived from balloon-borne tracer measurements in the 1999/2000 Arctic winter, Atmos. Chem. Phys., 5, 1423–1436, 2005, http://www.atmos-chem-phys.net/5/1423/2005/.

Ross, D. E. M., Pyle, J. A., Harris, N. R. P., McIntyre, J. D., Millard, G. A., Robinson, A. D., and Busen, R.: Investigation of Arctic ozone depletion sampled over midlatitudes during the Egrett campaign of spring/summer 2000, Atmos. Chem. Phys., 4, 1407–1417, 2004, http://www.atmos-chem-phys.net/4/1407/2004/.

Schmidt, U., Bauer, R., Engel, A., Borchers, R., and Lee, J., The variation of available chlorine Cly in the arctic polar vortex during EASOE, Geophys. Res. Lett., 21, 1215–1218, 1994.

Tienpont, B., David, F., Witdouck, W., and Sandra, P., Development of a miniature gas chromatograph (μCAD) with sample Enrichment, Programmed Temperature GC and Plasma Emission Detection, LC/GC Europe, 22, 112–124, 2009.

Urban, J., Lautie, N., Le Flochmoen, E., Jimenez, C., Eriksson, P., de La Noe, J., Dupuy, E., El Amraoui, L., Frisk, U., Jegou, F., Murtagh, D., Olberg, M., Ricaud, P., Camy-Peyret, C., Dufour, G., Payan, S., Huret, N., Pirre, M., Robinson, A. D., Harris, N. R. P., Bremer, H., Kleinbohl, A., Kullmann, K., Kunzi, K., Kuttippurath, J., Ejiri, M., Nakajima, H., Sasano, Y., Sugita, T., Yokota, T., Piccolo, C., Raspollini, P., and. Ridolfi, M.: Odin/SMR Limb Observations of Stratospheric Trace Gases: Validation of N_2O, J. Geophys. Res., 110, D09301, doi:10.1029/2004JD005394, 2005.

Volk, C. M. Elkins, J. W., Fahey, D. W., Salawitch, R. J., Dutton, G. S., Gilligan, J. M., Proffitt, M. H., Loewenstein, M., Podolske, J. R., Minschwaner, K., Margitan, J. J., and Chan, K. R., Quantifying Transport Between the Tropical and Mid-Latitude Lower Stratosphere, Science, 272, 1763–1768, doi:10.1126/science.272.5269.1763, 1996.

Worton, D.R., Mills, G. P., Oram, D. E., and Sturges, W. T.: Gas chromatography negative ion chemical ionisation mass spectrometry: Application to the detection of alkyl nitrates and halocarbons in the atmosphere, J. Chromatogr. A, 1201, 112–119, doi:10.1016/j.chroma.2008.06.019, 2008.